

Controlled Growth of Semiconducting and Metallic Single-Wall Carbon Nanotubes

Chang Liu* and Hui-Ming Cheng*

Shenyang National Laboratory for Materials Science, Institute of Metal Research, Chinese Academy of Sciences, Shenyang 110016, China

ABSTRACT: Single-wall carbon nanotubes (SWCNTs) can be either semiconducting or metallic depending on their chiral angles and diameters. The use of SWCNTs in electronics has long been hindered by the fact that the as-prepared SWCNTs are usually a mixture of semiconducting and metallic ones. Therefore, controlled synthesis of SWCNTs with a uniform electrical type or even predefined chirality has been a focus of carbon nanotube research in recent years. In this Perspective, we summarize recent progress on the controlled growth of semiconducting and metallic SWCNTs by *in situ* selective etching and by novel catalyst design. The advantages and mechanisms of these approaches are analyzed, and the challenges are discussed. Finally, we predict possible breakthroughs and future trends in the controlled synthesis and applications of SWCNTs.

■ INTRODUCTION

A single-wall carbon nanotube (SWCNT) can be imagined to be a seamless one-dimensional tubular structure rolled up from a single graphene layer.¹ Due to their unique atom-thick graphitic layer and very strong C–C bonding, SWCNTs demonstrate excellent properties, such as ultrahigh strength and Young's modulus, good chemical stability, high thermal and electrical conductivity, and high carrier mobility.² It is particularly intriguing that a SWCNT can be either semiconducting or metallic depending on its chiral angle and diameter, i.e., chirality.³ It has been experimentally and theoretically demonstrated that metallic SWCNTs (m-SWCNTs) can endure ultrahigh current densities due to ballistic electron transport, while semiconducting SWCNTs have high current on/off ratios and high carrier mobilities.⁴ Therefore, s-SWCNTs can be an ideal channel material for field effect transistors (FETs), and m-SWCNTs can be used as electrodes and interconnectors in circuits and for the fabrication of transparent conductive films (TCFs). Due to their nanosize, environmental friendliness, and excellent electrical and mechanical properties, SWCNTs are expected to be used in SWCNT-based computers⁵ and various flexible electronic devices with unprecedented excellent performance which may lead to revolutionary changes to human life and the development of society.⁶ However, the use of SWCNTs in electronics has long been hindered by the fact that the as-prepared SWCNTs are usually a mixture of semiconducting and metallic tubes, which degrades device performance and causes serious nonuniformity. The electrical properties of SWCNTs are very sensitive to their structures, i.e., the way that carbon atoms are assembled along the tube axis. A slight change of chiral angle or diameter will lead

to changes in the semiconducting/metallic features of a SWCNT. Usually, there are $\sim 2/3$ semiconducting and $\sim 1/3$ metallic nanotubes in an as-prepared SWCNT sample, and it is very difficult to achieve perfect structure and property control, due to their very similar structures and formation energies.² Therefore, the selective growth of s- and m-SWCNTs has been a focus of CNT research in recent years.

There are basically two approaches to obtaining SWCNTs of a uniform electrical type. The first is postsynthesis separation, where the mixed s- and m-SWCNTs are separated based on the differences in their physical and chemical properties, for example, by gradient density centrifugation,^{7,8} electric current breakdown,^{5,9} gel-based chromatography,¹⁰ and selective polymer interactions.¹¹ With the use of these methods, high purity s- and m-SWCNTs or even SWCNTs with specific chiralities can be obtained. However, due to the involvement of complex chemical and physical treatment processes and the introduction of chemicals for sample dispersion and separation, the SWCNTs produced are usually cut short, defective, and contaminated.^{12,13} As a result, devices fabricated from these SWCNTs show degraded properties.¹⁴ In addition, the preparation efficiency and yield of SWCNTs using this approach is extremely low, which limits scale-up production. Therefore, it is more desirable to prepare SWCNTs of a uniform type by another strategy, i.e., direct growth. The as-grown SWCNTs, without further separation treatment, are of good crystallinity and contain fewer defects, and are, therefore, more suitable for electronic and optoelectronic devices. The difficulty of synthesizing SWCNTs using the direct growth approach lies in the control of the structures and properties of SWCNTs during their growth process, which usually occurs at high temperatures and in a complex environment containing a catalyst, carbon source and carrier gas, and the formation energies and stabilities of s- and m-SWCNTs are very similar.

In this article, we summarize recent progress on the direct growth of s- and m-SWCNTs by *in situ* selective etching and by novel catalyst design. The selective growth mechanisms of the SWCNTs are analyzed, and the challenges remaining are discussed. Finally, we suggest the future trends in the controlled synthesis and uses of s- and m-SWCNTs.

■ GROWTH OF S- AND M-SWCNTS BY *IN SITU* SELECTIVE ETCHING

Although the structures of s- and m-SWCNTs are quite similar, their chemical stabilities are different. Liu et al. studied the dependence of the chemical stability of SWCNTs on their

Received: January 24, 2016

Published: May 5, 2016

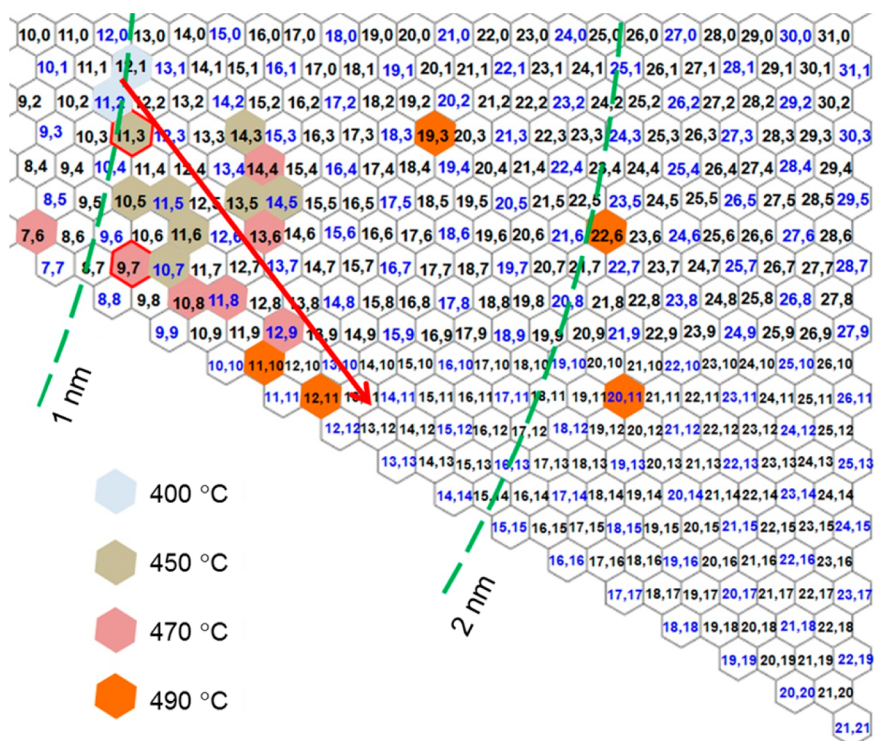


Figure 1. Chirality-dependent stability of SWCNTs as determined by the oxidation of individual SWCNTs at different temperatures. As indicated by the arrow, semiconducting, large diameter, and high-chiral-angle SWCNTs are chemically more stable. Reproduced with permission from ref 15. Copyright 2013 Wiley.

chiralities using transmission electron microscopy (TEM).¹⁵ The chirality of SWCNTs was determined by electron diffraction, and their chemical stability was evaluated by oxidation in air at different temperatures and subsequent observation under TEM. It was found that semiconducting, large diameter SWCNTs are chemically more stable (Figure 1). This is because the ionization potential of m-SWCNTs is higher than that of their semiconducting counterpart, and that the C–C bonds are evidently weakened for small diameter SWCNTs due to their higher curvature.^{16,17} Therefore, m-SWCNTs and small diameter s-SWCNTs may be preferentially removed by chemical etching. Here, “etching” means that SWCNTs with lower chemical stability in a sample preferentially react with an introduced etchant by forming carbon oxides or hydrocarbons and are removed selectively from the sample. Compared to the postsynthesis treatment methods, *in situ* selective etching is more desirable because the removal of newly nucleated SWCNTs around catalyst nanoparticles is easier and more cost-efficient.¹⁸ This is because better contact between etchant and newly grown SWCNTs (before bundling) can be achieved for the *in situ* etching. In addition, the active metal catalyst may also accelerate the etching process.

To achieve the selective growth of SWCNTs by etching, introduction of appropriate etchants is essential. Ding et al. grew aligned s-SWCNTs on a quartz substrate by chemical vapor decomposition (CVD) from mixed ethanol and methanol using Cu as catalyst.¹⁹ It can be seen from Figure 2a–d that the SWCNTs are well-aligned, densely packed, straight, and uniform in diameter. Figure 2e–f shows radial breathing mode (RBM) band Raman spectra of the sample excited with 633 and 488 nm lasers. The s-SWCNT content was found to be ~95%. It was proposed that the HO radicals originating from the methanol carbon source play a key role as an etchant to preferentially

remove m-SWCNTs, and this was supported by the fact that no semiconducting and metallic selectivity was observed when only ethanol was used as the carbon source. In addition, the selective growth of s-SWCNTs only applies to the aligned nanotubes with a very narrow diameter distribution, which facilitates efficient selective etching of m-SWCNTs. Water vapor was also used as an etchant to selectively remove m-SWCNTs.^{20,21} Zhou et al. achieved direct growth of s-SWCNTs on both quartz and silicon substrates, and the content of s-SWCNTs reached ~97%.²⁰ It was proposed that a suitable amount of moisture and a low carbon feed rate are essential to ensure that the growth rate of the m-SWCNTs is lower than the etching rate, so that the sample is enriched with s-SWCNTs. Che et al. reported the growth of s-SWCNTs on a quartz substrate using an isopropyl alcohol carbon stock.²² Mass spectrometry studies revealed that water vapor existed in the reactor. The water originating from the decomposition of isopropyl alcohol which acts as an etchant for m-SWCNTs. Rather than using a gas phase etchant, Qin et al. prepared s-SWCNTs on a Si substrate using a CeO₂ catalyst support, which released oxygen at elevated temperatures to obtain an oxidative environment and efficiently eliminated m-SWCNTs.²³ Hong et al. prepared s-SWCNTs (~95%) on a quartz substrate by applying UV beam irradiation.¹⁸ It was proposed that the UV irradiation leads to the formation of free radicals, which preferentially react and remove the as-formed caps of m-SWCNTs, thus resulting in the enrichment of s-SWCNTs. Although it is generally accepted that free radicals play a key role in the selective etching process, more detailed characterization is needed. It would be more desirable to realize *in situ* observation of the etching process of m-SWCNTs, which provides direct evidence and useful kinetics of the selective removal.

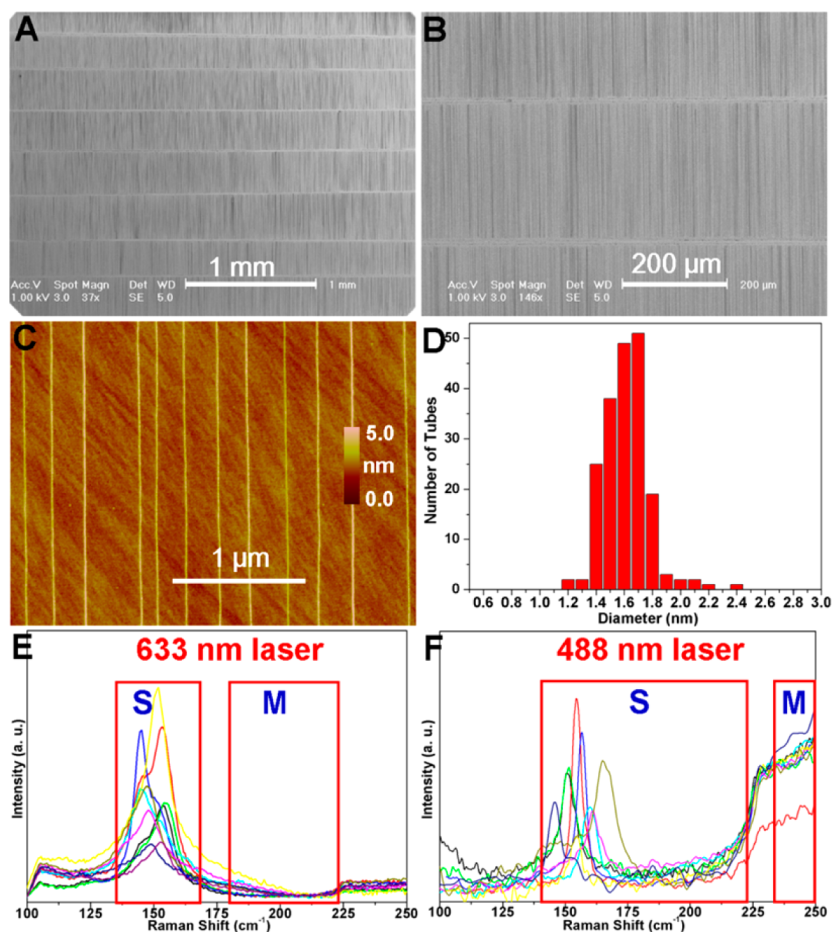


Figure 2. Arrays of almost exclusively semiconducting SWCNTs obtained using mixed ethanol and methanol as carbon source. (A and B) SEM images. (C) AFM image. (D) Diameter distribution of 200 SWCNTs of an array measured by AFM. (E and F) Raman spectra of the SWCNTs transferred onto a SiO_x/Si substrate. Each colored curve in (E) and (F) shows a spectrum measured at one spot of the sample. The rectangles marked with “S” and “M” denote the frequency ranges of RBM peaks of semiconducting and metallic SWCNTs, respectively. Reproduced with permission from ref 19. Copyright 2009 American Chemical Society.

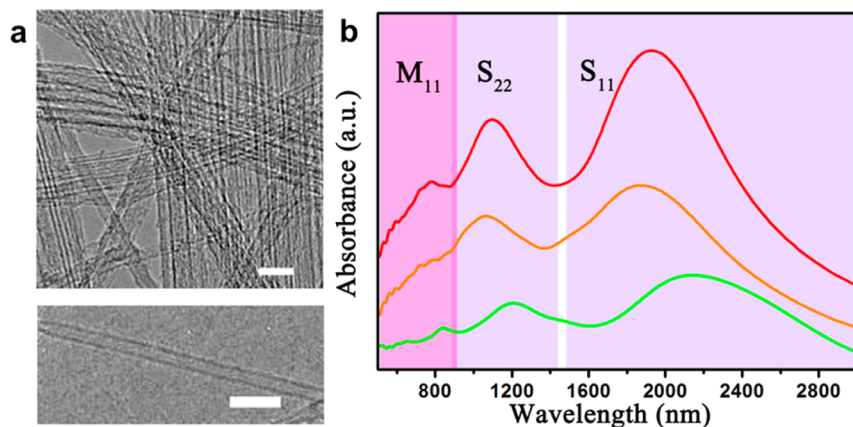


Figure 3. (a) TEM images and (b) absorption spectra of the SWCNTs prepared by FCCVD with a suitable amount of O_2 introduced. It can be seen that the SWCNTs are dominated by high-quality semiconducting nanotubes. Scale bar: 10 nm. The labels S_{11} and S_{22} indicate the excitonic optical absorption bands of s-SWCNTs, and the M_{11} label corresponds to the first-order transition of m-SWCNTs. Reproduced with permission from ref 27. Copyright 2011 American Chemical Society.

The above studies focus on the direct growth of s-SWCNTs on the substrate surface. The advantage of these surface-grown SWCNTs is that the position and alignment of the nanotubes are controllable, but the disadvantage is that the amount of SWCNTs grown is very limited, usually invisible to the naked

eye. For the fabrication of large-area thin film FETs (TFTs) and TCFs, there is a great demand for the large-scale synthesis of high quality s- and m-SWCNTs.

The floating catalyst CVD (FCCVD) method is one of the most efficient techniques for the growth of SWCNTs.^{24,25} The

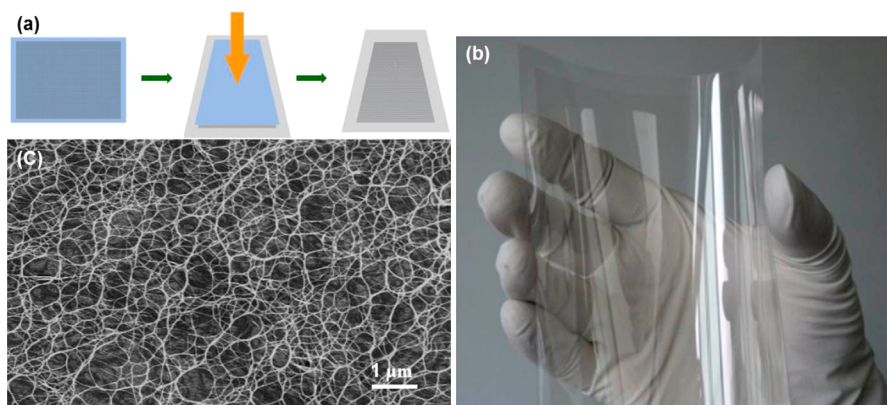


Figure 4. (a) A flowchart showing the dry transfer of as-prepared s-/m-SWCNTs by selective etching-FCCVD to a target substrate. (b) Optical image of a SWCNT-based TCF transferred onto a flexible PET substrate. (c) Typical SEM image of a self-assembled SWCNT thin film. Reproduced with permission from ref 30. Copyright 2014 American Chemical Society.

SWCNTs prepared are usually pure, straight, long, and highly crystalline.²⁶ Because the catalyst nanoparticles are in a floating state during the growth of the SWCNTs, it is much easier and efficient for the growing nanotubes to make good contact with the environmental gases and consequently to achieve selective etching. We have developed a selective etching-floating catalyst approach²⁷ in which a small amount of O₂ was introduced. The sample obtained was characterized by TEM and absorption spectroscopy (Figure 3), from which it can be seen that the SWCNTs are pure and straight and that the absorption peaks originating from the m-SWCNTs are evidently weakened at an optimum condition.²⁷ TFT performance and laser Raman measurements further confirmed the enrichment of s-SWCNTs in the as-prepared sample, and their content reached ~90%. Because oxygen is a strong oxidant, the optimum window for the selective growth of s-SWCNTs is very limited, and too much or too little oxygen leads to complete removal of either all SWCNTs or poor selectivity. In addition, the oxygen also tends to introduce defects in the surviving s-SWCNTs. We have, therefore, explored a milder gas phase etchant of H₂.²⁸ It was demonstrated that the introduction of an appropriate amount of hydrogen during the growth of SWCNTs by FCCVD can selectively remove m-SWCNTs, and the content of s-SWCNTs was shown to be ~93% by absorption spectroscopy. In addition, the temperature for the rapid oxidation of the s-SWCNTs was as high as 800 °C, indicating their very high quality. It was proposed that H₂ could be partially decomposed to free radicals at a high temperature of 1100 °C in the presence of the iron catalyst nanoparticles, and these free radicals then preferentially react with the m-SWCNTs.

These studies have achieved selective growth of s-SWCNTs based on the principle that m-SWCNTs are chemically more reactive than the semiconducting ones when they have similar diameters. Therefore, the selective growth of m-SWCNTs by etching is more difficult. Zhang et al. reported the synthesis of m-SWCNTs by postsynthesis gas phase etching using SO₃ as etchant.²⁹ However, the mechanism of this process is still unclear. Hou et al. intentionally synthesized SWCNTs containing small diameter s-SWCNTs and large diameter m-SWCNTs by tuning the synthesis parameters of FCCVD,³⁰ and hydrogen was introduced as an etchant. As a result, the small diameter s-SWCNTs were selectively removed, and a m-SWCNT-enriched (~88%) sample was obtained. A large-area m-SWCNT film was directly collected from the reactor (Figure 4). The transparent conductive performance of the m-SWCNT

film was much higher than that of SWCNTs without any selectivity for electrical type.

The selective etching-floating catalyst CVD permits large-scale, continuous synthesis of high-quality s- and m-SWCNTs controllably. The as-prepared SWCNTs can be directly collected in a form of thin films by using filters or rolled up substrates without any solution process (Figure 4a). Thus, high quality, large-area s- and m-SWCNTs can be prepared (Figure 4b,c) and used for the fabrication of various SWCNT-based high-performance devices, such as integrated TFTs and TCFs. For the selective etching-FCCVD approach, it is important to further improve the content of s-/m-SWCNTs in the samples obtained, which depends largely on the selection and optimization of the etchant used.

■ GROWTH OF S- AND M-SWCNTS BY CATALYST DESIGN

As mentioned above, *in situ* etching is an efficient method for the selective synthesis of high quality s- and m-SWCNTs. However, since the stability of a SWCNT is related to both its electrical type and diameter, and the grown SWCNTs usually have a range of diameters, it is difficult to obtain highly pure s-/m-SWCNTs by selective etching due to competition between the stabilities of electrical types and tube diameters. Therefore, to achieve precise control over the electrical type and even the chirality of SWCNTs, it is important to perform catalyst design and engineering, since the nucleation and growth of SWCNTs originate from the catalyst nanoparticles and their structures and properties are closely related to the catalyst used. The most commonly used catalysts for SWCNT growth are transition metals, such as iron, nickel and cobalt, which catalyze the growth of SWCNTs by the vapor–liquid–solid (VLS) mechanism with high efficiency.³¹ However, the samples obtained usually show no selectivity and contain both s- and m-SWCNTs with a wide range of diameters.²⁴ Although pioneer work on controlling the growth of SWCNTs according to their electrical type and chirality has been performed using morphology-tuned Fe³² and bimetallic Ni_xFe_{1-x}^{33,34} nanoparticles as catalysts, the detailed mechanisms are still not clear. Therefore, the search for novel catalysts for the selective growth of SWCNTs is highly important, and a thorough understanding of the growth mechanisms of SWCNTs will undoubtedly provide useful hints for the catalyst design.

Tang et al. studied the growth process and mechanism of SWCNTs using an *in situ* TEM technique³⁵ as schematically shown in Figure 5. They prepared multiwall CNTs (MWCNTs)

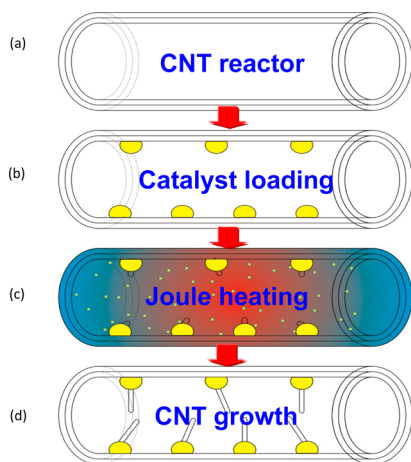


Figure 5. Schematic showing the experimental procedure of the *in situ* TEM method for investigating the growth mechanism of CNTs. (a) Preparation of a CNT with both open ends by the AAO template method. (b) Loading of catalyst NPs inside the hollow core of the CNT. (c) Nucleation of small CNTs driven by Joule heating and electron beam irradiation inside the TEM. (d) Growth of small CNTs from the catalyst NPs. Reproduced with permission from ref 35. Copyright 2014 American Chemical Society.

with open ends by an anodic aluminum oxide template method;³⁶ catalyst nanoparticles were then loaded inside the hollow core of the MWCNTs by wet chemical immersion, CVD, or thermal sublimation. With the aid of a TEM-STM holder, a voltage was applied to individual MWCNTs placed in the TEM chamber and the Joule heating effect induced high temperatures in the MWCNT nanofurnace. As a result, CNT growth occurred from the catalyst loaded inside the MWCNTs and the process was observed *in situ* under TEM. It was found that the morphology, composition, and solid/liquid states of the traditional iron catalyst changed during CNT growth, which explains why uniform traditional catalyst nanoparticles grow SWCNTs of random electrical types and chiralities.³⁵ On the other hand, when SWCNTs grow from catalysts having high melting points, such as SiO_x ³⁷ and BN,³⁸ the structure of these catalysts was observed not to change during the whole growth process. Therefore, novel highly stable catalysts may be more suitable for the structure-controlled growth of SWCNTs. In fact, carbonaceous nanostructures and high melting point alloys have been used for the controlled growth of SWCNTs very recently.

Yao et al. first reported “cloning” growth of SWCNTs using shortened SWCNTs as growth seeds.³⁹ The lengths of the original short SWCNTs were apparently elongated after CVD growth from ethanol. The chirality of the newly grown SWCNTs was characterized to be the same as that of the SWCNT seeds. This result indicates that the structure and property of SWCNTs can be inherited from parent carbonaceous catalysts. Liu et al. also performed “cloning” growth by using SWCNT seeds with a specific chirality prepared by postsynthesis separation,⁴⁰ and chirality-pure SWCNTs with an average length of $34.5 \mu\text{m}$, about 100 times that of the original seeds, were obtained.⁴¹ Liu et al. also reported a strategy that combines bottom-up organic chemistry synthesis and vapor phase epitaxy elongation.⁴² They first prepared $\text{C}_{50}\text{H}_{10}$ molecules as the cap of SWCNTs, then

performed CVD growth of SWCNTs using a mixture of CH_4 and C_2H_4 as the carbon source. As a result, small diameter s-SWCNTs were obtained, and selective etching produced by introducing H_2O was considered to play an important role. Sanchez-Valencia et al. synthesized a $\text{C}_{96}\text{H}_{54}$ precursor, which can be transformed to short (6, 6) SWCNT seeds after annealing at 500°C on a Pt(111) substrate.⁴³ By CVD from ethylene or ethanol, pure (6, 6) metallic SWCNTs with lengths of hundreds of nanometers were obtained. These results demonstrate that by designing and preparing a seed with a predefined structure, e.g., the cap of SWCNTs or a segment of SWCNTs for cloning, SWCNTs with a uniform electrical type or even chirality can be obtained. However, the yield and growth rate of SWCNTs from the carbonaceous seeds are very low, and the fine structure at the interface between the growth seeds and newly grown SWCNTs need further investigations.

Except for carbons, high melting-point alloys, metal carbides, and metal oxides have been explored for the controlled growth of SWCNTs. Yang et al. prepared tungsten-based alloys such as WCo, WFe, and WNi nanoparticles as catalysts for the templated growth of SWCNTs with specific structures and properties (Figure 6).⁴⁴ Due to their high melting-points, these alloy

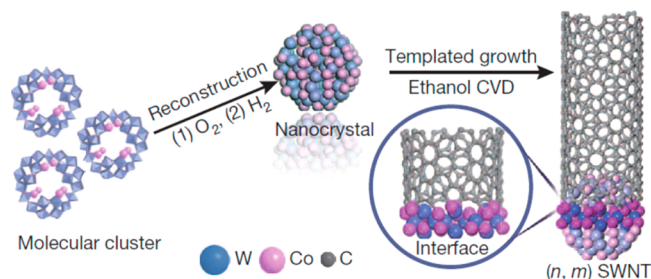


Figure 6. Preparation of W–Co catalyst and the templated growth of a SWCNT with specified chirality. Reproduced with permission from ref 44. Copyright 2014 Nature Publishing Groups.

nanoparticles retained their solid state and crystalline structure even at CVD growth temperatures over 1000°C . As a result, the content of (12, 6) metallic SWCNTs in the sample catalyzed by a WCo catalyst was shown to be $\sim 92\%$. Both *in situ* and *ex situ* TEM observations were performed to understand the reason for this unprecedented chirality-selective growth. It was found that W_6Co_7 nanoparticles kept their crystalline structure with facets when heated in vacuum up to 1100°C . Postsynthesis TEM observations revealed that the (12, 6) nanotube axis was perpendicular to the (0 0 12) plane of W_6Co_7 . DFT simulations confirmed a perfect geometrical match for the (12, 6) tube and the (0 0 12) plane of W_6Co_7 . Furthermore, by using W_6Co_7 catalysts containing an enrichment of (1 1 6) planes, the same group also achieved preferential growth of (16, 0) s-SWCNTs.⁴⁵ It is, therefore, suggested that a structural match between catalyst and nanotube might be an essential factor in the chirality-selective growth of SWCNTs. Very recently, Zhang et al. reported the growth of s-SWCNTs with a narrow diameter distribution using hexagonal Mo_2C nanoparticles as catalyst (Figure 7).⁴⁶ Figure 7a illustrates the procedure of obtaining a uniform Mo_2C catalyst from the precursor and the following growth of horizontal SWCNT arrays. A typical SEM image of the as-grown long, aligned SWCNTs is shown in Figure 7b. The RBM Raman peaks excited with a 514 nm laser appeared mainly at $\sim 190 \text{ cm}^{-1}$. Therefore, the SWCNTs were assigned as s-SWCNTs according to the Kataura plot.⁴⁷ It was proposed that

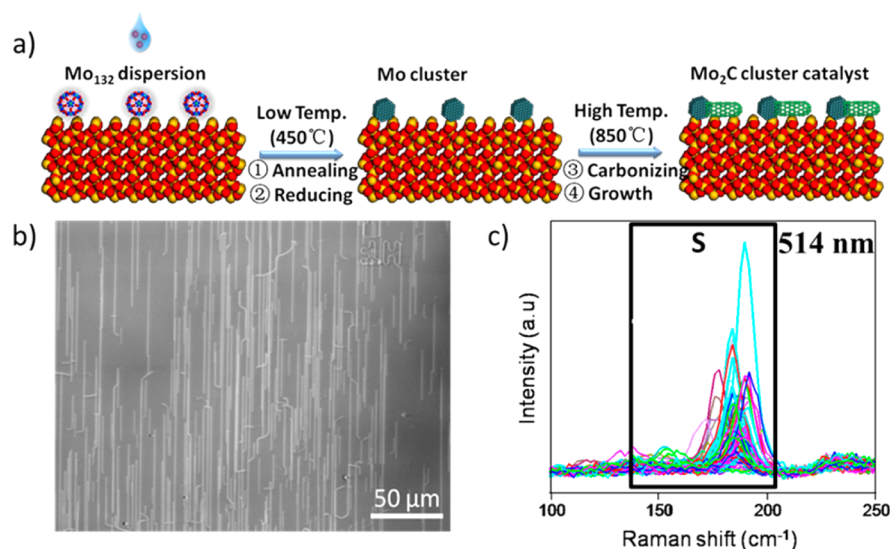


Figure 7. (a) Illustration of the growth of horizontally aligned s-SWCNT arrays using Mo_2C catalysts on a quartz substrate. (b) SEM image of a Mo_2C -catalyzed SWCNT array. (c) Raman spectra in the RBM region of the nanotubes transferred to a Si/SiO₂ (300 nm) substrate measured with a 514 nm laser. A linear scan was performed over a distance of 200 μm with a step of 1 μm , and each colored curve shows a spectrum measured at one spot. The black rectangle labeled with “S” presents the RBM region of s-SWCNTs detectable using the 514 nm laser. Reproduced with permission from ref 46. Copyright 2015 American Chemical Society.

the Mo_2C nanoparticles selectively catalyze the scission of the C–O bond of ethanol, and the resultant O radicals preferentially etch metallic nanotubes; thus, s-SWCNTs with a narrow diameter and chirality distribution were obtained. Kang et al. reported the growth of s-SWCNT arrays using oxygen-deficient TiO_2 nanoparticles as catalyst.⁴⁸ Theoretical calculations showed that TiO_2 nanoparticles with oxygen vacancies have a lower formation energy for s-SWCNTs than that for m-SWCNTs, thus achieving the preferential growth of s-SWCNTs with a high content of ~95%. High melting-point alloy/compound catalysts have shown great potential for growing SWCNTs with specific structures; however, the controllable growth mechanism is still unclear.

■ SUMMARY AND PROSPECTS

As mentioned above, notable progress has been made on the synthesis of s- and m-SWCNTs in terms of high purity,^{42–44} high quality,^{28,30} and controllable packing configurations⁴⁹ by either *in situ* selective etching or novel catalyst design.⁵⁰ However, there are big challenges to be faced. First, the purity of s-/m-SWCNTs prepared by *in situ* selective etching needs to be further improved. *In situ* selective etching has been demonstrated to be an effective approach to prepare s- and m-SWCNTs in bulk, based on the principle that the chemical stabilities of these two types of SWCNTs are different. The best reported contents of s- and m-SWCNTs obtained in bulk by selective etching are ~93%²⁸ and ~88%,³⁰ respectively. Since the stability of a SWCNT is related to both its electrical type and diameter, it is important to grow SWCNTs with a very narrow diameter distribution to achieve high-content s-/m-SWCNTs. To achieve this objective, the design and preparation of well-dispersed, and stable catalyst nanoparticles of the same size is essential. Therefore, the combination of selective etching and novel catalyst design may be a feasible way to achieve high-content s-/m-SWCNTs. As an example, very recently, Zhang et al. designed and prepared a uniform, monodispersed partially carbon-coated Co nanoparticle catalyst (Figure 8a) using a block copolymer self-assembly method,⁵¹ where the carbon coating functions to both prevent

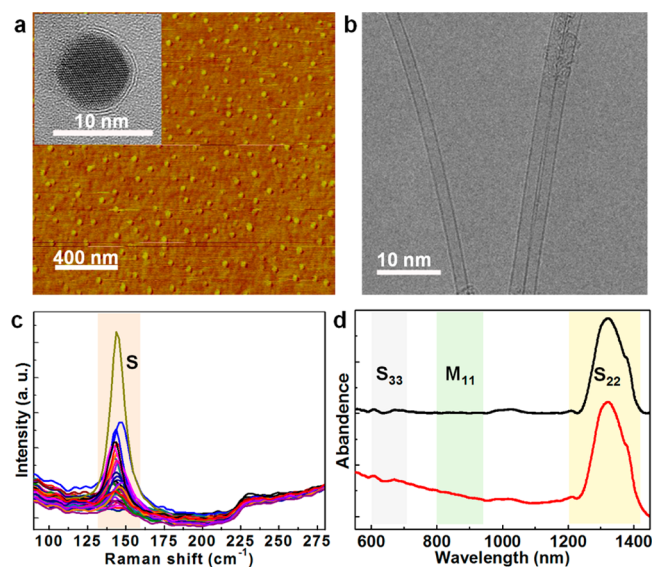


Figure 8. (a) AFM image of partially carbon-coated Co nanoparticles. The inset is high resolution TEM image showing the structure of a catalyst nanoparticle. (b) Typical TEM image of the SWCNTs grown from the partially carbon-coated Co catalyst. (c) RBM Raman spectra of the as-grown SWCNTs excited with 532 nm laser. (d) Absorption spectra of the SWCNTs. Red line, as-collected curve; black line, curve with background subtracted. Reproduced with permission from ref 51. Copyright 2016 Nature Publishing Groups.

the aggregation of encapsulated Co nanoparticles and guarantee a perpendicular growth mode of SWCNTs from the exposed Co. As a result, the SWCNTs grown have high quality and a very uniform diameter (Figure 8b). When H_2 was used as an *in situ* growth etchant, high purity s-SWCNTs with narrow diameter- and band gap distributions were obtained as characterized by multiwavelength Raman spectra and absorption (Figure 8c,d). Furthermore, the currently used etchants for the selective growth of SWCNTs include mainly O_2 ,²⁷ H_2O ,²⁰ H_2 ,²⁸ and methanol that may produce reactive radicals. If more efficient and “smart”

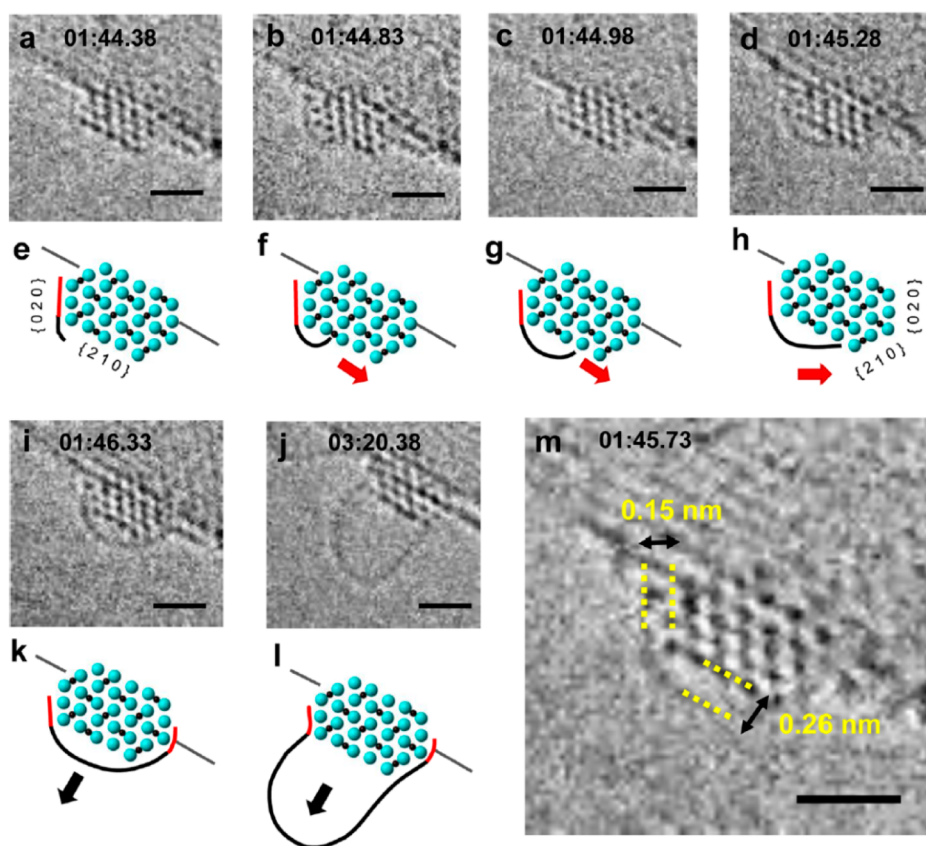


Figure 9. *In situ* time-resolved TEM images and models of SWCNT nucleation and growth. (a–d, i, and j) A series of images showing SWCNT growth from Co_2C . (e–h, k, and l) Corresponding atomic models. The active surfaces of the catalyst are identified as $\{020\}$ and $\{210\}$. (m) Snapshot showing the average distances between the growing structure and the $\{020\}$ and $\{210\}$ catalyst surfaces before nanotube lift-off. Scale bars are 1 nm. Reproduced with permission from ref 52 Copyright 2014 American Chemical Society.

etchants particularly toward *s*-/*m*-SWCNTs can be developed, the purity of *s*-/*m*-SWCNTs would be further improved.

Second, the working mechanisms of novel catalysts and their design principles need further investigation. Exciting progress has been made on the chirality-controlled growth of SWCNTs using high melting-point alloys⁴⁴ and structure-defined carbon caps.⁴³ To improve the growth efficiency by this approach and to achieve better controllability, it is important to thoroughly understand their growth mechanisms. Although efforts have been made, and possible growth mechanisms have been proposed based on experimental and simulation results, more direct evidence showing the correlation between the structure of the catalysts and the chirality of grown SWCNTs are greatly needed. It seems possible to get valuable hints and information on this matter using *in situ* TEM SWCNT growth, since the lattice structure of catalysts can be well-defined and the chirality of SWCNTs can be determined by electron diffraction. Pitcher et al. performed atomically resolved imaging of the nucleation of SWCNTs from Co_2C nanoparticles in an environmental TEM⁵² and found that the incorporation of additional carbon atoms leads to cap lift-off on the (210) plane and nanotube growth, while the sides stay anchored to the $\{020\}$ surfaces (Figure 9). Because the cap structure is controlled by nanoparticle facet geometry, the chirality of the SWCNTs will also be determined at this stage.

He et al. also observed the formation of SWCNT caps from Co nanoparticles with well-resolved crystalline fringes in an environmental TEM.⁵³ In addition, they reported the prefer-

ential growth of *s*-SWCNTs in an ambient CO atmosphere because the epitaxial Co nanoparticles promote high chiral selectivity. Although valuable results have been obtained in the above studies, a relationship between the chirality of the SWCNTs and the catalyst could not be given, possibly because that the *in situ* grown SWCNTs are very short and it is difficult to determine their chiralities by electron diffraction. In trying to reveal the correlation between the structures of the catalysts and the grown SWCNTs using the *in situ* TEM growth approach, there may be difficulties originating from the low catalytic activity of these novel catalysts (compared to normal transition metals) and the low hydrocarbon pressure allowed in an environmental TEM chamber, which prevent the growth of SWCNTs with good crystallinity and sufficient length for diffraction characterization. Innovation in equipment, such as environmental TEMs and atmospheric environmental cells, would further facilitate these *in situ* TEM studies. On the other hand, theoretical studies, that have proven efficient in predicting and interpreting the growth process and structure of SWCNTs, may play an important role in the design of novel catalysts and in revealing the interactions between SWCNTs and catalysts at the nucleation and growth stages.^{54–59} A combination of *in situ* TEM studies and theoretical predictions could bring new insight to the catalytic growth of SWCNTs. The clarification of the growth mechanisms and the design principles of novel high melting-point catalysts will hopefully further promote the structure- and property-controlled growth of SWCNTs.

Third, standardized methods for accurately characterizing the contents of *s*-/*m*-SWCNTs need to be established. The structures of *s*- and *m*-SWCNTs are quite similar, and it is difficult to differentiate these two types of SWCNTs using normal characterization techniques. Thus, to establish reliable methods for determining the contents of *s*-/*m*-SWCNTs in a sample is essential for understanding the controlled growth of SWCNTs. Currently, *s*-/*m*-SWCNTs can be characterized using multiwavelength laser Raman spectroscopy,^{23,32,48} absorption spectroscopy,^{27,60,61} fluorescence spectroscopy,^{62,63} electron diffraction,^{64,65} SEM observation,⁶⁶ and the performance of fabricated FETs.^{42,46,67} However, each of these techniques may be applicable to some specific SWCNT samples and may have its advantages and limitations. For example, absorption spectroscopy measurements require a large quantity of SWCNTs and reflect macro-scale statistical results. To determine the chirality of SWCNTs by electron diffraction, the nanotubes must be isolated, straight and clean, but the number of SWCNTs that can be examined is very limited. Fluorescence spectroscopy provides the chirality distribution of a large sample quantity, but is only valid for *s*-SWCNTs. Currently, researchers have to use 2 to 3 or even more techniques to measure the content of *s*-/*m*-SWCNTs so that comprehensive and reliable results are obtained. Because of the variety of SWCNT samples in terms of quantity, crystallinity, size, growth substrate, and configuration, the issue of *s*-/*m*-SWCNT content measurements is still far from well addressed. A possible solution is to define standard samples with a series of contents of *s*-/*m*-SWCNTs and diameters, and their standard Raman/absorption/fluorescence spectra determined. These standard samples could be prepared by postsynthesis separation and/or direct growth with their structures thoroughly characterized. Then, their typical Raman spectra, absorption spectra and fluorescence spectra could be measured and recorded as standard spectra. By comparing spectra from a new sample with the standard samples, the contents of *s*-/*m*-SWCNTs in a sample could be determined. Anyway, to achieve the establishment of convenient, accurate, sensitive, and reliable standard characterization methods, great effort is still needed.

With further improvements in the controlled synthesis of *s*-/*m*-SWCNTs, we may expect to see their practical applications in the near future. However, the fabrication of next-generation SWCNT-based computers requires *s*-SWCNTs with both very high purity ($\geq 99.9999\%$) and high packing density (>125 isolated tubes/ μm) and appropriate processing techniques need to be developed to ensure high performance and good reliability, and therefore, this may take a considerably long time.⁶⁸ The use of enriched *s*-SWCNTs in thin film FETs and the use of enriched *m*-SWCNTs in transparent conductive films can hopefully be achieved in a few years. In these cases, the fabrication of high-quality, large-area, highly uniform *s*-/*m*-SWCNT films is of great importance. Recent reports have demonstrated that SWCNTs prepared by the floating catalyst CVD method can be directly collected through a gas phase approach to form large-area films.^{30,69} By combining *in situ* selective etching, floating catalyst CVD growth, and gas phase collection techniques, high quality *s*-/*m*-SWCNT films may be obtained on a large scale. For use in flexible electronics, SWCNT film-based devices have the advantages of excellent flexibility, good stability and desirable electrical and optical properties compared to traditional materials and other newly emerging competitors. Therefore, these high quality *s*-/*m*-SWCNT films can hopefully find uses in TCFs, TFTs and various flexible devices in the next few years.

In summary, the direct synthesis of *s*- and *m*-SWCNTs is a focus of CNT research and a bottleneck for the use of CNTs in electronics. Notable progress has been made using the *in situ* selective etching and novel catalyst design approaches in recent years. Parallel *s*-SWCNT arrays with a purity of $\sim 97\%$ ²⁰ and free-standing *m*-SWCNT thin films with a purity of $\sim 88\%$ ³⁰ have been prepared. To further improve the purity and controllability of *s*- and *m*-SWCNTs, it is essential to more clearly understand the selective growth and etching mechanisms of SWCNTs, so that more efficient catalysts and etchants can be discovered. The combination of catalyst design and selective etching could be a feasible and efficient way of doing this. These selectively grown *s*- and *m*-SWCNTs can hopefully be used in TFTs, TCFs, and advance the development of flexible electronics in the near future.

AUTHOR INFORMATION

Corresponding Authors

*cliu@imr.ac.cn

*cheng@imr.ac.cn

Notes

The authors declare no competing financial interest.

ACKNOWLEDGMENTS

This work was supported by the Ministry of Science and Technology of China (Grant 2011CB932601), the National Natural Science Foundation of China (Grants 51521091, 51172241, 51532008, and 51272257), the Chinese Academy of Sciences (Grant KGZD-EW-T06), the CAS/SAFEA International Partnership Program for Creative Research Teams, and the Liaoning BaiQianWan Talents Program.

REFERENCES

- (1) Jorio, A.; Dresselhaus, G.; Dresselhaus, M. S. *Carbon Nanotubes*; Springer: Berlin Heidelberg, 2008.
- (2) Saito, R.; Dresselhaus, G.; Dresselhaus, M. S. *Physical Properties of Carbon Nanotubes*; World Scientific: London, 1998.
- (3) Saito, R.; Fujita, M.; Dresselhaus, G.; Dresselhaus, M. S. *Appl. Phys. Lett.* **1992**, *60*, 2204.
- (4) Odom, T. W.; Huang, J. L.; Kim, P.; Lieber, C. M. *Nature* **1998**, *391*, 62.
- (5) Shulaker, M. M.; Hills, G.; Patil, N.; Wei, H.; Chen, H. Y.; PhilipWong, H. S.; Mitra, S. *Nature* **2013**, *501*, 526.
- (6) Park, S.; Vosguerichian, M.; Bao, Z. A. *Nanoscale* **2013**, *5*, 1727.
- (7) Arnold, M. S.; Green, A. A.; Hulvat, J. F.; Stupp, S. I.; Hersam, M. C. *Nat. Nanotechnol.* **2006**, *1*, 60.
- (8) Ghosh, S.; Bachilo, S. M.; Weisman, R. B. *Nat. Nanotechnol.* **2010**, *5*, 443.
- (9) Collins, P. C.; Arnold, M. S.; Avouris, P. *Science* **2001**, *292*, 706.
- (10) Liu, H. P.; Nishide, D.; Tanaka, T.; Kataura, H. *Nat. Commun.* **2011**, *2*, 309.
- (11) Nish, A.; Hwang, J. Y.; Doig, J.; Nicholas, R. J. *Nat. Nanotechnol.* **2007**, *2*, 640.
- (12) Ding, J. F.; Li, Z.; Lefebvre, J.; Cheng, F. Y.; Dubey, G.; Zou, S.; Finnie, P.; Hrdina, A.; Scoles, L.; Lopinski, G. P.; Kingston, C. T.; Simard, B.; Malenfant, P. R. L. *Nanoscale* **2014**, *6*, 2328.
- (13) Wang, H.; Yuan, Y.; Wei, L.; Goh, K.; Yu, D. S.; Chen, Y. *Carbon* **2015**, *81*, 1.
- (14) LeMieux, M. C.; Sok, S.; Roberts, M. E.; Opatkiewicz, J. P.; Liu, D.; Barman, S. N.; Patil, N.; Mitra, S.; Bao, Z. *ACS Nano* **2009**, *3*, 4089.
- (15) Liu, B. L.; Jiang, H.; Krashennikov, A. V.; Nasibulin, A. G.; Ren, W. C.; Liu, C.; Kauppinen, E. I.; Cheng, H. M. *Small* **2013**, *9*, 1379.
- (16) Tasis, D.; Tagmatarchis, N.; Bianco, A.; Prato, M. *Chem. Rev.* **2006**, *106*, 1105.

- (17) Lu, J.; Nagase, S.; Zhang, X. W.; Wang, D.; Ni, M.; Maeda, Y.; Wakahara, T.; Nakahodo, T.; Tsuchiya, T.; Akasaka, T.; Gao, Z. X.; Yu, D. P.; Ye, H. Q.; Mei, W. N.; Zhou, Y. S. *J. Am. Chem. Soc.* **2006**, *128*, 5114.
- (18) Hong, G.; Zhang, B.; Peng, B. H.; Zhang, J.; Choi, W. M.; Choi, J. Y.; Kim, J. M.; Liu, Z. F. *J. Am. Chem. Soc.* **2009**, *131*, 14642.
- (19) Ding, L.; Tselev, A.; Wang, J. Y.; Yuan, D. N.; Chu, H. B.; McNicholas, T. P.; Li, Y.; Liu, J. *Nano Lett.* **2009**, *9*, 800.
- (20) Zhou, W.; Zhan, S.; Ding, L.; Liu, J. *J. Am. Chem. Soc.* **2012**, *134*, 14019.
- (21) Li, P.; Zhang, J. *J. Mater. Chem.* **2011**, *21*, 11815.
- (22) Che, Y.; Wang, C.; Liu, J.; Liu, B.; Lin, X.; Parker, J.; Beasley, C.; Wong, H. S. P.; Zhou, C. *ACS Nano* **2012**, *6*, 7454.
- (23) Qin, X. J.; Peng, F.; Yang, F.; He, X. H.; Huang, H. X.; Luo, D.; Yang, J.; Wang, S.; Liu, H. C.; Peng, L. M.; Li, Y. *Nano Lett.* **2014**, *14*, 512.
- (24) Cheng, H. M.; Li, F.; Su, G.; Pan, H. Y.; He, L. L.; Sun, X.; Dresselhaus, M. S. *Appl. Phys. Lett.* **1998**, *72*, 3282.
- (25) Cheng, H. M.; Li, F.; Sun, X.; Brown, S. D. M.; Pimenta, M. A.; Marucci, A.; Dresselhaus, G.; Dresselhaus, M. S. *Chem. Phys. Lett.* **1998**, *289*, 602.
- (26) Liu, Q. F.; Ren, W. C.; Chen, Z. G.; Wang, D. W.; Liu, B. L.; Yu, B.; Li, F.; Cong, H. T.; Cheng, H. M. *ACS Nano* **2008**, *2*, 1722.
- (27) Yu, B.; Liu, C.; Hou, P. X.; Tian, Y.; Li, S. S.; Liu, B. L.; Li, F.; Kauppinen, E. I.; Cheng, H. M. *J. Am. Chem. Soc.* **2011**, *133*, 5232.
- (28) Li, W. S.; Hou, P. X.; Liu, C.; Sun, D. M.; Yuan, J. T.; Zhao, S. Y.; Yin, L. C.; Cong, H. T.; Cheng, H. M. *ACS Nano* **2013**, *7*, 6831.
- (29) Zhang, H. L.; Liu, Y. Q.; Cao, L. C.; Wei, D. C.; Wang, Y.; Kajiuira, H.; Li, Y. M.; Noda, K.; Luo, G. F.; Wang, L.; Zhou, J.; Lu, J.; Gao, Z. X. *Adv. Mater.* **2009**, *21*, 813.
- (30) Hou, P. X.; Li, W. S.; Zhao, S. Y.; Li, G. X.; Shi, C.; Liu, C.; Cheng, H. M. *ACS Nano* **2014**, *8*, 7156.
- (31) Jourdain, V.; Bichara, C. *Carbon* **2013**, *58*, 2.
- (32) Harutyunyan, A. R.; Chen, G. G.; Paronyan, T. M.; Pigos, E. M.; Kuznetsov, O. A.; Hewaparakrama, K.; Kim, S. M.; Zakharov, D.; Stach, E. A.; Sumanasekera, G. U. *Science* **2009**, *326*, 116.
- (33) Chiang, W. H.; Sankaran, R. M. *Nat. Mater.* **2009**, *8*, 882.
- (34) Chiang, W. H.; Sakr, M.; Gao, X. P. A.; Sankaran, R. M. *ACS Nano* **2009**, *3*, 4023.
- (35) Tang, D. M.; Liu, C.; Yu, W. J.; Zhang, L. L.; Hou, P. X.; Li, J. C.; Li, F.; Bando, Y.; Golberg, D.; Cheng, H. M. *ACS Nano* **2014**, *8*, 292.
- (36) Hou, P. X.; Yu, W. J.; Shi, C.; Zhang, L. L.; Liu, C.; Tian, X. J.; Dong, Z. L.; Cheng, H. M. *J. Mater. Chem.* **2012**, *22*, 15221.
- (37) Liu, B. L.; Ren, W. C.; Gao, L. B.; Li, S. S.; Pei, S. F.; Liu, C.; Jiang, C. B.; Cheng, H. M. *J. Am. Chem. Soc.* **2009**, *131*, 2082.
- (38) Tang, D. M.; Zhang, L. L.; Liu, C.; Yin, L. C.; Hou, P. X.; Jiang, H.; Zhu, Z.; Li, F.; Liu, B. L.; Kauppinen, E. I.; Cheng, H. M. *Sci. Rep.* **2012**, *2*, 971.
- (39) Yao, Y.; Feng, C.; Zhang, J.; Liu, Z. *Nano Lett.* **2009**, *9*, 1673.
- (40) Tu, X. M.; Manohar, S.; Jagota, A.; Zheng, M. *Nature* **2009**, *460*, 250.
- (41) Liu, J.; Wang, C.; Tu, X. M.; Liu, B. L.; Chen, L.; Zheng, M.; Zhou, C. W. *Nat. Commun.* **2012**, *3*, 1199.
- (42) Liu, B. L.; Liu, J.; Li, H. B.; Bhola, R.; Jackson, E. A.; Scott, L. T.; Page, A.; Irle, S.; Morokuma, K.; Zhou, C. W. *Nano Lett.* **2015**, *15*, 586.
- (43) Sanchez-Valencia, J. R.; Dienel, T.; Groning, O.; Shorubalko, I.; Mueller, A.; Jansen, M.; Amsharov, K.; Ruffieux, P.; Fasel, R. *Nature* **2014**, *512*, 61.
- (44) Yang, F.; Wang, X.; Zhang, D. Q.; Yang, J.; Luo, D.; Xu, Z. W.; Wei, J. K.; Wang, J. Q.; Xu, Z.; Peng, F.; Li, X. M.; Li, R. M.; Li, Y. L.; Li, M. H.; Bai, X. D.; Ding, F.; Li, Y. *Nature* **2014**, *510*, 522.
- (45) Yang, F.; Wang, X.; Zhang, D. Q.; Qi, K.; Yang, J.; Xu, Z.; Li, M. H.; Zhao, X. L.; Bai, X. D.; Li, Y. *J. Am. Chem. Soc.* **2015**, *137*, 8688.
- (46) Zhang, S. C.; Tong, L. M.; Hu, Y.; Kang, L. X.; Zhang, J. *J. Am. Chem. Soc.* **2015**, *137*, 8904.
- (47) Kataura, H.; Kumazawa, Y.; Maniwa, Y.; Umezumi, I.; Suzuki, S.; Ohtsuka, Y.; Achiba, Y. *Synth. Met.* **1999**, *103*, 2555.
- (48) Kang, L. X.; Hu, Y.; Liu, L. L.; Wu, J. X.; Zhang, S. C.; Zhao, Q. C.; Ding, F.; Li, Q. W.; Zhang, J. *Nano Lett.* **2015**, *15*, 403.
- (49) Hu, Y.; Kang, L. X.; Zhao, Q. C.; Zhong, H.; Zhang, S. C.; Yang, L. W.; Wang, Z. Q.; Lin, J. J.; Li, Q. W.; Zhang, Z. Y.; Peng, L. M.; Liu, Z. F.; Zhang, J. *Nat. Commun.* **2015**, *6*, 6099.
- (50) Zhang, J.; Terrones, M.; Park, C. R.; Mukherjee, R.; Monthioux, M.; Koratkar, N.; Kim, Y. S.; Hurt, R.; Frackowiak, E.; Enoki, T.; Chen, Y.; Chen, Y. S.; Bianco, A. *Carbon* **2016**, *98*, 708.
- (51) Zhang, F.; Hou, P. X.; Liu, C.; Wang, B. W.; Jiang, H.; Chen, M. L.; Sun, D. M.; Li, J. C.; Cong, H. T.; Kauppinen, E. I.; Cheng, H. M. *Nat. Commun.* **2016**, *7*, 11160.
- (52) Picher, M.; Lin, P. A.; Gomez-Ballesteros, J. L.; Balbuena, P. B.; Sharma, R. *Nano Lett.* **2014**, *14*, 6104.
- (53) He, M. S.; Jiang, H.; Liu, B. L.; Fedotov, P. V.; Chernov, A. I.; Obratsova, E. D.; Cavalca, F.; Wagner, J. B.; Hansen, T. W.; Anoshkin, I. V.; Obratsova, E. A.; Belkin, A. V.; Sairanen, E.; Nasibulin, A. G.; Lehtonen, J.; Kauppinen, E. I. *Sci. Rep.* **2013**, *3*, 1460.
- (54) Ding, F.; Larsson, P.; Larsson, J. A.; Ahuja, R.; Duan, H. M.; Rosen, A.; Bolton, K. *Nano Lett.* **2008**, *8*, 463.
- (55) Artyukhov, V. I.; Penev, E. S.; Yakobson, B. I. *Nat. Commun.* **2014**, *5*, 4892.
- (56) Yuan, Q. H.; Ding, F. *Angew. Chem., Int. Ed.* **2015**, *54*, 5924.
- (57) Ding, F.; Harutyunyan, A. R.; Yakobson, B. I. *Proc. Natl. Acad. Sci. U. S. A.* **2009**, *106*, 2506.
- (58) Penev, E. S.; Artyukhov, V. I.; Yakobson, B. I. *ACS Nano* **2014**, *8*, 1899.
- (59) Pigos, E.; Penev, E. S.; Ribas, M. A.; Sharma, R.; Yakobson, B. I.; Harutyunyan, A. R. *ACS Nano* **2011**, *5*, 10096.
- (60) Luo, Z. T.; Pfefferle, L. D.; Haller, G. L.; Papadimitrakopoulos, F. *J. Am. Chem. Soc.* **2006**, *128*, 15511.
- (61) Lee, H. W.; Yoon, Y.; Park, S.; Oh, J. H.; Hong, S.; Liyanage, L. S.; Wang, H. L.; Morishita, S.; Patil, N.; Park, Y. J.; Park, J. J.; Spakowitz, A.; Galli, G.; Gygi, F.; Wong, P. H. S.; Tok, J. B. H.; Kim, J. M.; Bao, Z. A. *Nat. Commun.* **2011**, *2*, 541.
- (62) Wang, H.; Wang, B.; Quek, X. Y.; Wei, L.; Zhao, J. W.; Li, L. J.; Chan-Park, M. B.; Yang, Y. H.; Chen, Y. A. *J. Am. Chem. Soc.* **2010**, *132*, 16747.
- (63) Mistry, K. S.; Larsen, B. A.; Blackburn, J. L. *ACS Nano* **2013**, *7*, 2231.
- (64) Zhu, Z.; Jiang, H.; Susi, T.; Nasibulin, A. G.; Kauppinen, E. I. *J. Am. Chem. Soc.* **2011**, *133*, 1224.
- (65) He, M. S.; Liu, B. L.; Chernov, A. I.; Obratsova, E. D.; Kauppi, I.; Jiang, H.; Anoshkin, I.; Cavalca, F.; Hansen, T. W.; Wagner, J. B.; Nasibulin, A. G.; Kauppinen, E. I.; Linnekoski, J.; Niemela, M.; Lehtonen, J. *Chem. Mater.* **2012**, *24*, 1796.
- (66) Li, J.; He, Y. J.; Han, Y. M.; Liu, K.; Wang, J. P.; Li, Q. Q.; Fan, S. S.; Jiang, K. L. *Nano Lett.* **2012**, *12*, 4095.
- (67) Zhang, G. Y.; Qi, P. F.; Wang, X. R.; Lu, Y. R.; Li, X. L.; Tu, R.; Bangsaruntip, S.; Mann, D.; Zhang, L.; Dai, H. J. *Science* **2006**, *314*, 974.
- (68) Franklin, A. D. *Nature* **2013**, *498*, 443.
- (69) Sun, D. M.; Timmermans, M. Y.; Tian, Y.; Nasibulin, A. G.; Kauppinen, E. I.; Kishimoto, S.; Mizutani, T.; Ohno, Y. *Nat. Nanotechnol.* **2011**, *6*, 156.